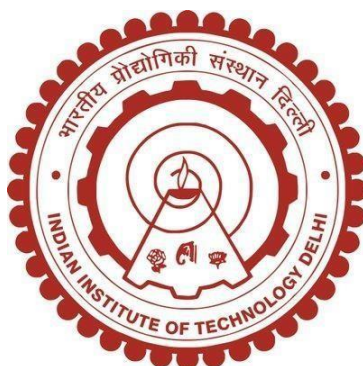


**RAFT AGENT PRIMED MESOPOROUS SILICA PARTICLES
FOR SELECTIVE GRAFTING OF POLYMER CHAINS AND
THEIR APPLICATIONS**

SMRUTIREKHA MISHRA



DEPARTMENT OF MATERIALS SCIENCE AND ENGINEERING

INDIAN INSTITUTE OF TECHNOLOGY

OCTOBER 2021

©Indian Institute of Technology Delhi (IITD), New Delhi, 2021

**RAFT AGENT PRIMED MESOPOROUS SILICA PARTICLES
FOR SELECTIVE GRAFTING OF POLYMER CHAINS AND
THEIR APPLICATIONS**

by

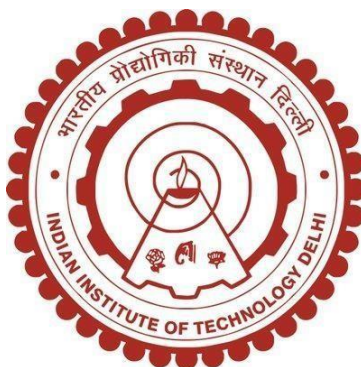
SMRUTIREKHA MISHRA

Department of Materials Science and Engineering

Submitted

in fulfillment of the requirements of the degree of Doctor of Philosophy

to the



**INDIAN INSTITUTE OF TECHNOLOGY
OCTOBER 2021**

CERTIFICATE

This is to certify that the thesis entitled “***RAFT AGENT PRIMED MESOPOROUS SILICA PARTICLES FOR SELECTIVE GRAFTING OF POLYMER CHAINS AND THEIR APPLICATIONS***” being submitted by Ms. Smrutirekha Mishra to the Indian Institute of Technology Delhi for the award of degree of Doctor of Philosophy is a record of bonafide research work carried out by her. Ms. Smrutirekha Mishra has worked under my guidance and supervision and has fulfilled the requirements for the submission of her thesis, which to our knowledge has reached the requisite standard.

The results contained in this thesis are original and have not been submitted, in part or full, to any University or Institute for the award of any degree or diploma.



Dr. Leena Nebhani

Associate Professor

Department of Materials Science and Engineering

Indian Institute of Technology Delhi

Hauz Khas, New Delhi, India-110016.

ACKNOWLEDGMENTS

I will be always thankful to my guide Prof. Leena Nebhani for giving me the opportunity to work with her. Her philosophical approach of explaining things, intrigued me for exploring more ideas directly or indirectly related to this thesis work. During this up and down of PhD journey her constant encouragement generated the interest to overcome hurdles and progress further.

I will be always obliged to the Department of Materials Science and Engineering for providing the necessary equipment and facilities required to fulfill this thesis. I wish to express my gratitude to Head of the Department Prof Josemon Jacob for his support and suggestions. I would also like to thank my PhD committee members; Prof Anup K. Ghosh and Prof. Rajiv Srivastava for their inspiration and constructive criticism throughout my research work. Furthermore, I would like to thank Prof. S.N. Maiti, Prof. Veena Choudhary, Prof. Rajesh Prasad, Prof. B.K. Satapathy, Prof. Jayant Jain, Prof. Sampa Saha, Prof. Suresh Neelakantan, Prof. Nitya Nand Goswami, Prof. B. K. Tripathi, Prof. Neerat Ray, Prof. Ankur Goswami, Prof. Laxmi Narayan R and Prof. Sangeeta Santra, for their invaluable support.

Sincere thanks to Prof. Bishwajit Kundu, School of Biological Science IIT Delhi for his time and allowing me to finish my biological application study in their lab. Many thanks to Prof. Cheng-Yu Wang, Associate Professor, NCTU Taiwan for allowing me work in his lab and learn new instrumentation techniques which will be cherished forever.

Most importantly, I am grateful to Mr. Surendra K. Sharma, Mr. Shivkant, Ms. Aastha Sharma and Mr. Alok Yadav for helping me to carry out all the characterization for my thesis work. My sincere thanks to Mr. Islam, Mr. Gajraj, Mr. Ashok Kapoor, Mrs. Shalini Arora, Mr. Amit, Mr. Pandey and all other office staff for their constant motivation.

I cannot forget to mention Surface and Macromolecular group members (Sumbul, Aanchal, Tina, Amit, Lukkumanul, Prathiba, Islam, Subhendu, Laxmi, Amit Patel, Desh Deepak, Dharmendra, Ahilan, Pushpa, Surya, Parna, Ramachandran, Omair, Pratim, Pramit) for their support always and making me smile through this up and down PhD journey. My seniors who have always been a support in any difficulty throughout this work, I will be grateful to Agni, Devendra, Savita ma'am and Shivangi ma'am. I will also grateful to all my other seniors (Sabapathy, Anindya, Reshu) and juniors (Shaifali, Aishwaria, Ashok, Biswajit, Shivani, Harshal, Ankit) who have directly or indirectly helped me always through this journey.

Friends who are more than family have always stood by side as constant support, thank you Mamata, Nitu, Sushant, Sagarika, Aarti, Bariya and Shikha.

In addition, I would like to give my special thanks to the special person of my life Mr. Panigrahi, for his silent dedication to me for all these years and I hope I will become a punctual person like you someday.

Thanks to my family members; my father, mother and in-laws who have been a constant support to keep me mentally and physically fit through this journey. Last but not the least I am always thankful to my god Jagannath for his blessings and giving me the strength to become who I am.

Smrutirekha Mishra

This thesis is dedicated to my Father
(Mr. B.N Mishra)

*“Fears are unseen, his love is unexpected, but his care and protection will remain as a pillar
of strength throughout our lives”*

-John C. Maxwell

ABSTRACT

Cutting-edge achievements have been made towards controlled synthesis of different types of mesoporous silica nanoparticles (MSNs) using variety of structure directing agents. The possibility of organically functionalizing interior and exterior surfaces of MSNs utilizing various organoalkoxysilanes is one of the most interesting and challenging areas in the field of surface engineering today. MSN's superlative properties such as high surface area, ordered pore structure and uniform pore size distribution has been the motivation for further modification, functionalization, and application of MSNs. Thus, depending on the functional organic groups present inside or outside the surface of MSNs, they have been widely used in catalysis, sensors, absorbents, and drug delivery. The main pathway for these processes includes post functionalization in which an organic group is covalently attached to the inorganic surface after the synthesis of the MSNs, or by co-condensation which involves incorporation of the organic group during the synthesis of MSNs. Utilizing these pathways further for the surface modification of MSNs with polymers can alter the inherent properties of the MSNs and makes it compatible for different applications.

In this thesis, we have performed synthesis of RAFT agent functionalized MSNs *via* co-condensation and further grafting of different polymers [poly(*N*-isopropyl acrylamide), poly(acrylic acid) and poly(acrylamide)] from RAFT primed MSNs *via* surface initiated RAFT polymerization was carried out. Further, these polymers grafted MSNs were utilized for controlled drug delivery and nanoconfinement of ammonia borane application studies. Two different types of organoalkoxysilane-based RAFT agent having two different types of R group such as isobutyric acid and phenylethyl group were synthesized and characterized by ^1H NMR, ^{13}C NMR and UV-visible spectroscopy. For the preparation of RAFT functionalized MSNs, different mmol % of both

organoalkoxysilane-based RAFT agent was chosen with respect to silica precursor (TEOS) such as 6, 12.8 and 18 mmol %. The synthesis of RAFT functionalized MSNs was confirmed by UV-visible spectroscopy, FTIR, TGA and solid-state NMR. The morphological analysis of the RAFT agent functionalized MSNs was carried out utilizing SEM and TEM. Different morphology of the RAFT agent functionalized MSNs was observed such as spherical shape for isobutyric acid group containing MSNs and short-rod shape for phenylethyl group containing MSNs. Following such morphological changes, it was also observed that isobutyric acid group containing RAFT agent were preferentially functionalized outside the surface of MSNs and phenylethyl group containing RAFT agent were preferentially functionalized inside the pores of MSNs. Consequently, different polymers (PNIPAM, PAA, PAM) were then grafted preferentially outside and inside the surface of MSNs.

To practically understand the applicability of the stimuli responsive polymers such as poly(*N*-isopropyl acrylamide), poly(acrylic acid) grafted MSNs, in-vitro loading and release of drug doxorubicin (Dox) was performed at different pH and temperature. Further ex-vivo assay was performed in MCF-7 cancerous cell line of the Dox loaded polymer-grafted MSNs. An efficient Dox loading was observed in both cases of PAA and PNIPAM grafted MSNs. In-vitro Dox release from both the systems was demonstrated effectively via changing pH or temperature of the surrounding environment. The cell viability assay clearly showed the pH responsiveness of the PAA chains allows the release of Dox at pH 7.4 with a good efficacy to kill MCF-7 cells. From these studies, it was concluded that polymer-grafted MSNs synthesized from in-built RAFT agent containing MSNs can be effectively used in different therapeutic applications.

Similarly, poly(acrylamide) grafted MSNs were efficiently utilized as an organic-inorganic hybrid material for nanoconfinement of AB. The nanoconfinement of AB was successful established by

FTIR, ^{11}B solid-state NMR, XPS and XRD. It was observed that dehydrogenation temperatures of AB confined MSNs generally agreed with theoretical predicted trend based on surface tension provided by nanoconfinement. However, AB nanoconfined in PAM-COOH-MSNs had even lower dehydrogenation temperature. This was observed possibly due to synergistic effect of AB nanosize, as well as strong interaction between AB and the functional groups present in these inorganic structures which was proved by XPS. For justifying the effect, kinetics at temperature near to the T_d was also performed and it was observed that higher equivalent of hydrogen was released at temperature near to T_d from AB confined PAM grafted MSNs. Hence, utilization of these polymer-grafted organically modified MSNs with active organic functional groups would possibly widen its window to be used as a catalyzing material for thermolysis of AB for generation of hydrogen.

सार

विभिन्न प्रकार के मेसोपोरस सिलिका नैनोकणों (MSNs) के नियंत्रित संश्लेषण की दिशा में अत्याधुनिक उपलब्धियां बनाई गई हैं, जो विभिन्न प्रकार के संरचना निर्देशन एजेंटों का उपयोग करती हैं। विभिन्न ऑर्गेनोकोक्सीसिलेंस का उपयोग करने वाले एमएसएन के आंतरिक और बाहरी सतहों को व्यवस्थित रूप से कार्यात्मक बनाने की संभावना आज सतह इंजीनियरिंग के क्षेत्र में सबसे दिलचस्प और चुनौतीपूर्ण क्षेत्रों में से एक है। एमएसएन के उच्च सतह क्षेत्र जैसे शानदार गुण, छिद्र संरचना और समान छिद्र आकार वितरण का आदेश दिया गया है जो एमएसएन के आगे संशोधन, कार्यात्मककरण और आवेदन के लिए प्रेरणा है। इस प्रकार, एमएसएन की सतह के अंदर या बाहर मौजूद कार्यात्मक कार्बनिक समूहों के आधार पर, उन्हें व्यापक रूप से कटैलिसिस, सेंसर, अवशोषक और दवा वितरण में उपयोग किया गया है। इन प्रक्रियाओं के लिए मुख्य मार्ग में पोस्ट फंक्शनलाइज़ेशन शामिल है जिसमें एमएसएन के संश्लेषण के बाद या सह-संघनन द्वारा एक कार्बनिक समूह को अकार्बनिक सतह से जोड़ा जाता है जिसमें एमएसएन के संश्लेषण के दौरान कार्बनिक समूह का समावेश शामिल होता है। पॉलिमर के साथ एमएसएन की सतह संशोधन के लिए इन मार्गों का आगे उपयोग करना एमएसएन के निहित गुणों को बदल सकता है और इसे विभिन्न अनुप्रयोगों के लिए संगत बनाता है।

इस थीसिस में, हमने RAFT एजेंट के संश्लेषण को सह-संक्षेपण के माध्यम से एमएसएन को कार्यात्मक बनाया है और सतह के माध्यम से विभिन्न पॉलिमर [पॉली (एन-आइसोप्रोपाइल एक्रिलामाइड), पॉली (एक्रिलिक एसिड) और पॉली (एक्रिलामाइड)] के आगे ग्राफ्टिंग किया है। आरएएफटी पोलीमराइजेशन शुरू किया गया। इसके अलावा, इन पॉलिमर ने एमएसएन को नियंत्रित दवा वितरण और अमोनिया बोरेन आवेदन अध्ययन के नैनोकॉनफाइन्मेंट के लिए उपयोग किया था। दो अलग-अलग प्रकार के ऑर्गेनोकोक्सीसिलीन-आधारित आरएएफटी एजेंट जिसमें दो अलग-अलग प्रकार के आर समूह होते हैं जैसे कि आइसोब्यूट्रिक एसिड और फिनाइलथाइल समूह को ^1H NMR, ^{13}C NMR और UV-दृश्यमान स्पेक्ट्रोस्कोपी द्वारा संश्लेषित और विशेषता दी गई थी। आरएएफटी कार्यात्मक एमएसएन की तैयारी के लिए, दोनों के अलग-अलग मिमील %organoalkoxysilane- आधारित RAFT एजेंट को सिलिका अग्रदूत (TEOS) जैसे 6, 12.8 और 18 mmol% के संबंध में चुना गया था। आरएएफटी कार्यात्मक एमएसएन के संश्लेषण की पुष्टि यूवी-दृश्य स्पेक्ट्रोस्कोपी द्वारा की गई थी। एफटीआईआर, टीजीए और ठोस राज्य एनएमआर। RAFT एजेंट कार्यात्मक एमएसएन का रूपात्मक विश्लेषण SEM और TEM का उपयोग करके किया गया था। RAFT एजेंट के विभिन्न आकारिकी कार्यात्मक एमएसएन को देखा गया जैसे कि आइसोब्यूट्रिक एसिड समूह के लिए गोलाकार आकार जिसमें एमएसएन और फेनिलथाइल समूह युक्त एमएसएन के लिए शॉर्ट-रॉड आकार शामिल है। इस तरह के रूपात्मक परिवर्तनों के बाद, यह भी देखा गया कि RAFT एजेंट वाले आइसोब्यूट्रिक एसिड समूह को एमएसएन की सतह के बाहर अधिमानतः कार्यात्मक किया गया था और आरएएफटी एजेंट युक्त फिनाइलथाइल समूह एमएसएन के छिद्रों के अंदर अधिमानतः

कार्यात्मक थे। नतीजतन, विभिन्न पॉलिमर (PNIPAM, PAA, PAM) तब एमएसएन की सतह के बाहर और अंदर अधिमानतः ग्राफ्ट किए गए थे।

पॉली (एन- आइसोप्रोपिल एक्रिलामाइड), पॉली (एक्रेलिक एसिड) ग्राफ्टेड एमएसएन, इन-विट्रो लोडिंग और ड्रग डॉक्सोर्बिसिन (डॉक्स) की रिहाई के लिए व्यावहारिक रूप से उत्तेजना के प्रति उत्तरदायी पॉलिमर की प्रयोज्यता को समझने के लिए अलग-अलग पीएच और तापमान पर प्रदर्शन किया गया था। आगे पूर्व-विवो परख को DO_x लोड किए गए बहुलक-ग्राफ्टेड MSNs के MCF-7 कैंसर सेल लाइन में किया गया था। पीएच और पीएनआईपीएम ग्राफ्टेड एमएसएन के दोनों मामलों में एक कुशल डॉक्स लोडिंग देखी गई। दोनों प्रणालियों से इन-विट्रो डॉक्स रिलीज को आसपास के वातावरण के पीएच या तापमान को बदलने के माध्यम से प्रभावी ढंग से प्रदर्शित किया गया था। सेल व्यवहार्यता परख ने स्पष्ट रूप से पीएच श्रृंखलाओं की पीएच जवाबदेही को दिखाया जो एमसीएफ -7 कोशिकाओं को मारने के लिए एक अच्छी प्रभावकारिता के साथ पीएच 7.4 पर डॉक्स को छोड़ने की अनुमति देता है। इन अध्ययनों से, यह निष्कर्ष निकाला गया कि एमएसएन युक्त इन-बिल्ट आरएएफटी एजेंट से संश्लेषित बहुलक-ग्राफ्टेड एमएसएन को विभिन्न चिकित्सीय अनुप्रयोगों में प्रभावी रूप से उपयोग किया जा सकता है।

इसी तरह, पॉली (एक्रिलामाइड) ग्राफ्टेड एमएसएन को एबी के नैनोकॉनफाइनमेंट के लिए एक कार्बनिक-अकार्बनिक संकर सामग्री के रूप में कुशलता से उपयोग किया गया था। एबी का नैनोकॉनफाइनमेंट सफल रहा।

एफटीआईआर, 11 बी ठोस-राज्य एनएमआर, एक्सपीएस और एक्सआरडी। यह देखा गया कि एबी के निर्जलीकरण तापमान ने एमएसएन को सीमित कर दिया है जो आमतौर पर नैनोकॉनफाइनमेंट द्वारा प्रदान की गई सतह तनाव के आधार पर सैद्धांतिक भविष्यवाणी की प्रवृत्ति से सहमत है। हालांकि, PAM-COOH-MSNs में AB नैनोकॉनफाइनमेंट में भी कम निर्जलीकरण तापमान था। यह संभवतः एबी नैनोसाइज के सहक्रियात्मक प्रभाव के कारण देखा गया था।, साथ ही एबी और इन अकार्बनिक संरचनाओं में मौजूद कार्यात्मक समूहों के बीच मजबूत बातचीत जो एक्सपीएस द्वारा साबित हुई थी। प्रभाव को सही ठहराने के लिए, टीडी के पास के तापमान पर कैनेटीक्स भी प्रदर्शन किया गया था और यह देखा गया था कि एबी से पीएएम सीमित एमएम ग्राफ्टेड एमएसएन के पास तापमान पर उच्च हाइड्रोजन के बराबर जारी किया गया था। इसलिए, सक्रिय कार्बनिक कार्यात्मक समूहों के साथ इन बहुलक-ग्राफ्टेड व्यवस्थित रूप से संशोधित एमएसएन का उपयोग संभवतः हाइड्रोजन की पीढ़ी के लिए एबी के थर्मोलिसिस के लिए एक उत्प्रेरित सामग्री के रूप में उपयोग की जाने वाली इसकी खिड़की को चौड़ा करेगा।

TABLE OF CONTENT

CERTIFICATE.....	i
ACKNOWLEDGMENTS.....	ii
ABSTRACT.....	v
LIST OF FIGURES.....	xviii
LIST OF TABLES.....	xxiii
LIST OF ABBREVIATIONS.....	xxv

Chapter 1. Introduction and Literature Review

1.1 Background and significance.....	2
1.2 Overview of mesoporous silica materials.....	4
1.3 Synthesis of mesoporous silica nanoparticles.....	6
1.4 Functionalization of mesoporous silica nanoparticles.....	12
1.4.1 Post-modification approach.....	12
1.4.2 Co-condensation approach.....	14
1.5 Functionalization of mesoporous silica nanoparticles using controlled radical polymerization.....	20
1.5.1 Atom transfer radical polymerization (ATRP).....	21
1.5.2 Reversible addition-fragmentation chain transfer (RAFT) polymerization.	24
1.5.3 Nitroxide-mediated polymerization (NMP).....	27
1.8. Characterization of polymer-grafted mesoporous silica nanoparticles.....	28
1.9. Applications of polymer functionalized mesoporous silica nanoparticles.....	30

1.10. Gap in literature and objective of the work.....	36
1.11 Thesis organization.....	37
1.12 References.....	40

Chapter 2. Synthesis and characterization of RAFT agent primed mesoporous silica nanoparticles

2.1. Introduction.....	47
2.2. Experimental.....	49
2.2.1. Characterization.....	49
2.2.2. Materials.....	51
2.2.3. Synthesis of organoalkoxysilane RAFT agent containing isobutyric acid as R group (RAFT-COOH).....	51
2.2.4. Synthesis of organoalkoxysilane RAFT agent containing phenyl ethyl as R group (RAFT-Ph).....	52
2.2.5. Stability study for organoalkoxysilane RAFT agent containing isobutyric acid as R group.....	52
2.2.6. Stability study for organoalkoxysilane RAFT agent containing phenyl ethyl as R group.....	53
2.2.7. Synthesis of control mesoporous silica nanoparticles (Control-MSNs).....	53
2.2.8. Synthesis of isobutyric acid R group containing organoalkoxysilane functionalized mesoporous silica nanoparticles (RAFT-COOH-MSNs).....	54
2.2.9. Synthesis of phenyl ethyl R group containing organoalkoxysilane functionalized mesoporous silica nanoparticles (RAFT-Ph-MSNs).....	54

2.3. Results and discussion.....	55
2.3.1. Characterization of organoalkoxysilane RAFT agent containing isobutyric acid as R group (RAFT-COOH).....	56
2.3.2. Characterization of organoalkoxysilane RAFT agent containing phenyl ethyl as R group (RAFT-Ph).....	58
2.3.3. Stability study for organoalkoxysilane RAFT agent containing isobutyric acid as R group (RAFT-COOH).....	60
2.3.4. Stability study for organoalkoxysilane RAFT agent containing phenyl ethyl as R group (RAFT-Ph).....	62
2.3.5. Characterization of RAFT agent primed MSNs (RAFT-COOH-MSNs).....	65
2.3.6. Characterization of organic-inorganic hybrid RAFT primed MSNs (RAFT-Ph-MSNs).....	73
2.3.7. Morphological characterization of RAFT primed MSNs (RAFT-COOH-MSNs and RAFT-Ph-MSNs).....	75
2.4. Conclusions.....	82
2.5. References.....	84

Chapter 3. Synthesis and characterization of poly(N-isopropyl acrylamide) and poly(acrylic acid) grafted mesoporous silica nanoparticles and its application in controlled drug delivery

3.1. Introduction.....	88
3.2. Experimental.....	90
3.2.1. Characterization.....	90

3.2.2. Materials.....	91
3.2.3. Synthesis of poly(N-isopropyl acrylamide) grafted MSNs from RAFT primed MSNs (PNIPAM-COOH-MSNs, PNIPAM-Ph-MSNs).....	92
3.2.4. Synthesis of poly(acrylic acid) grafted MSNs from RAFT primed MSNs (PAA-COOH-MSNs, PAA-Ph-MSNs).....	93
3.2.5. Determination of molecular weight by aminolysis for PNIPAM grafted MSNs and PAA grafted MSNs.....	94
3.2.6. In-vitro loading of doxorubicin into PNIPAM and PAA grafted MSNs (PNIPAM-COOH-MSNs, PNIPAM-Ph-MSNs, PAA-COOH-MSNs and PAA-Ph-MSNs).....	94
3.2.7. In-vitro release of doxorubicin from PNIPAM and PAA grafted MSNs (PNIPAM-COOH-MSNs, PNIPAM-Ph-MSNs, PAA-COOH-MSNs and PAA-Ph-MSNs).....	95
3.2.8. Ex-vivo cytotoxicity assay for PNIPAM and PAA grafted MSNs.....	95
3.2.9. Cellular uptake of PNIPAM and PAA grafted MSNs by confocal laser scanning microscopy.....	97
3.3. Results and discussion.....	97
3.3.1. Characterization of PNIPAM grafted MSNs (PNIPAM-COOH-MSNs and PNIPAM-Ph-MSNs).....	98
3.3.2. Characterization of PAA grafted MSNs (PAA-COOH-MSNs and PAA-Ph-MSNs).....	110
3.3.3. Application of PNIPAM and PAA grafted MSNs in controlled drug release	120
3.4. Conclusion.....	128

3.5. References.....	129
----------------------	-----

Chapter 4. Synthesis and characterization of poly(acrylamide) grafted mesoporous silica nanoparticles and its application in nanoconfinement of ammonia borane

4.1. Introduction.....	134
4.2. Experimental.....	138
4.2.1. Characterization.....	138
4.2.2. Materials.....	141
4.2.3. Synthesis of poly(acrylamide) grafted MSNs from RAFT primed MSNs (PAM-COOH-MSNs, PAM-Ph-MSNs).....	141
4.2.4. Synthesis of ammonia borane (AB) nanoconfined poly(acrylamide) grafted MSNs from RAFT primed MSNs (AB-PAM-COOH-MSNs and AB-PAM-Ph-MSNs).....	142
4.3. Results and discussion.....	143
4.3.1. Characterization of PAM grafted MSNs (PAM-COOH-MSNs and PAM-Ph-MSNs).....	143
4.3.3. Application of PAM grafted MSNs for nanoconfinement of ammonia borane and hydrogen release studies.....	151
4.4. Conclusion.....	163
4.5. References.....	164
Chapter 5. Conclusion and future outlook.....	169
Curriculum Vitae.....	173

LIST OF FIGURES

Figure 1.1	Structures of MS41 family mesoporous silica materials (a) MCM-41, (b) MCM-48 and (c) MCM-50.....	4
Figure 1.2	Structures of SBA family mesoporous silica materials (a) SBA-15 and (b) SBA-16.....	6
Figure 1.3	Sol-gel synthesis scheme of silica network by hydrolysis and condensation.....	8
Figure 1.4	General scheme for synthesis of mesoporous silica nanoparticles via surfactant template approach.....	10
Figure 1.5	Functionalization of MSNs via post-modification technique.....	13
Figure 1.6	Functionalization of MSNs via co-condensation approach.....	15
Figure 1.7	Different techniques for polymer grafting (a) Physically (Physisorption), (b) Grafting-to approach and (c) Grafting-from approach.....	19
Figure 1.8	General scheme for atom transfer radical polymerization.....	21
Figure 1.9	General scheme for reversible addition-fragmentation chain transfer polymerization.....	24
Figure 1.10	General scheme for nitroxide-mediated polymerization.....	27
Figure 2.1	¹ H NMR of organoalkoxysilane-based RAFT agent containing isobutyric acid as R group in CDCl ₃	57
Figure 2.2	¹³ C NMR of organoalkoxysilane-based RAFT agent containing isobutyric acid as R group in CDCl ₃	57
Figure 2.3	¹ H NMR of organoalkoxysilane-based RAFT agent containing phenyl ethyl as R group in CDCl ₃	59
Figure 2.4.	¹³ C NMR of organoalkoxysilane-based RAFT agent containing isobutyric acid as R group in CDCl ₃	59

Figure 2.5.	¹ H NMR spectra of RAFT-COOH at various stages of treatment a) RAFT-COOH before reaction with NaOH or HCl, b) RAFT-COOH after reaction with NaOH, c) RAFT-COOH after reaction with NaOH and HCl.....	61
Figure 2.6.	The UV-Visible spectra for RAFT-COOH, RAFT-COOH after treatment with NaOH and HCl showing absorption at 310 nm. The colour of the RAFT-COOH derives from the thiocarbonyl moiety, which absorbs light in the near UV range due to the allowed π - π^* transition.....	62
Figure 2.7	¹ H NMR spectra of RAFT-Ph at various stages of treatment a) RAFT-Ph before reaction with NaOH or HCl, b) RAFT-Ph after reaction with NaOH, c) RAFT-Ph after reaction with NaOH and HCl.....	64
Figure 2.8.	The UV-Visible spectra for RAFT-Ph RAFT-Ph after treatment with NaOH and HCl showing absorption at 310 nm. The colour of the RAFT-Ph derives from the thiocarbonyl moiety, which absorbs light in the near UV range due to the allowed π - π^* transition.....	65
Figure 2.9	Comparative FTIR spectra for control-MSNs, RAFT-COOH-MSNs6, RAFT-COOH-MSNs12.8 and RAFT-COOH-MSNs18.....	66
Figure 2.10	¹³ C solid state NMR spectra for a) RAFT-COOH-MSNs6, b) RAFT-COOH-MSNs12.8 and c) RAFT-COOH-MSNs18.....	67
Figure 2.11	TGA weight loss curve for RAFT-COOH-MSNs6, RAFT-COOH-MSNs12.8 and RAFT-COOH-MSNs18 in comparison to control-MSNs...	68
Figure 2.12	Comparative FTIR spectra for control-MSNs, RAFT-Ph-MSNs6, RAFT-Ph-MSNs12.8 and RAFT-Ph-MSNs18.....	71
Figure 2.13	¹³ C solid state NMR spectra for a) RAFT-Ph-MSNs6, b) RAFT-Ph-MSNs12.8 and c) RAFT-Ph-MSNs18.....	73
Figure 2.14	TGA weight loss curve for RAFT-Ph-MSNs6, RAFT-Ph-MSNs12.8 and RAFT-Ph-MSNs18 in comparison to control-MSNs.....	74
Figure 2.15	SEM micrographs for a) RAFT-COOH-MSNs6, b) RAFT-COOH-MSNs12.8 and c) RAFT-COOH-MSNs18.....	78
Figure 2.16	SEM micrographs for a) RAFT-Ph-MSNs6, b) RAFT-Ph-MSNs12.8 and c) RAFT-Ph-MSNs18.....	79

Figure 2.17	XPS wide scan for RAFT-COOH-MSNs ^{12.8} and RAFT-Ph-MSNs ^{12.8} in comparison to control-MSNs.....	80
Figure 2.18	Narrow scan for S2p XPS spectra for RAFT-COOH-MSNs ^{12.8}	81
Figure 3.1	FTIR spectra for a) PNIPAM-COOH-MSNs and b) PNIPAM-Ph-MSNs...	99
Figure 3.2	¹³ C solid state NMR spectra for a) PNIPAM-COOH-MSNs and b) PNIPAM-Ph-MSNs.....	100
Figure 3.3	TGA curve for a) PNIPAM-COOH-MSNs and b) PNIPAM-Ph-MSNs...	101
Figure 3.4	SEM for a) PNIPAM-Ph-MSNs having cuboid shape morphology and b) PNIPAM-COOH-MSNs having spherical shape morphology.....	105
Figure 3.5	TEM micrographs for a) PNIPAM-Ph-MSNs and b) PNIPAM-COOH-MSNs.....	105
Figure 3.6	(a) Wide scan for PNIPAM-COOH-MSNs in comparison to RAFT-COOH-MSNs and (b) Wide scan for PNIPAM-Ph-MSNs in comparison to RAFT-Ph-MSNs.....	107
Figure 3.7	a) C1s XPS spectra for PNIPAM-COOH-MSNs and b) N1s XPS spectra for PNIPAM-COOH-MSNs.....	108
Figure 3.8	FTIR spectra for a) PAA grafted MSNs from RAFT-COOH-MSNs and b) PAA grafted MSNs from RAFT-Ph-MSNs.....	110
Figure 3.9	Solid state ¹³ C NMR spectra for a) PAA-COOH-MSNs and b) PAA-Ph-MSNs.....	111
Figure 3.10	TGA weight loss for PAA-COOH-MSNs having total weight loss of 43.3 wt. % and PAA-Ph-MSNs with total weight loss of 34.7 wt. %.....	112
Figure 3.11	FESEM micrographs showing spherical shaped morphology for a) PAA-COOH-MSNs and b) cuboid shaped morphology for PAA-Ph-MSNs.....	116
Figure 3.12	TEM micrographs for a) PAA-Ph-MSNs and b) PAA-COOH-MSNs.....	117
Figure 3.13	Loading efficiency trend for both PNIPAM and PAA grafted MSNs.....	120
Figure 3.14	Release efficiency trend for a) PNIPAM-COOH-MSNs and b) PNIPAM-Ph-MSNs at different temperature and time period.....	121

Figure 3.15	Release efficiency trend for a) PAA-COOH-MSNs and b) PAA-Ph-MSNs at different pH and time period.....	122
Figure 3.16	MCF-7 percentage cell viability for both PNIPAM grafted MSNs through MTT assay upon exposure to different concentrations of MSNs as compared to control, showing no detrimental effect at any concentration.....	124
Figure 3.17	Percentage viability for MCF-7 cells incubated with different concentrations Dox-encapsulated MSNs as compared to free Dox. a) PAA grafted MSNs and b) PNIPAM grafted. Cells were incubated with the given concertation of MSNs in triplicate at 37°C and pH 7.4 for 48 h before analysis.....	125
Figure 3.18	Confocal microscopic images showing uptake of Dox loaded into PAA grafted MSNs by MCF-7 cells. Dark field microscopic images (A and B) free Dox alone (without cells) show clusters of smaller size with similar magnification and scale bar. (C and D) Dark field microscopic images of cells incubated with the respective Dox loaded PAA grafted MSNs showing efficient uptake. (E and F) Bright field images of the same cells. (G and H) Merged images of C, D, E and F.	128
Figure 4.1	FTIR spectra for a) PAM-COOH-MSNs and b) PAM-Ph-MSNs.....	140
Figure 4.2	¹³ C solid state NMR spectra for a) PAM-COOH-MSNs and b) PAM-Ph-MSNs.....	141
Figure 4.3	TGA plots for (a) PAM grafted from RAFT-COOH-MSNs and (b) PAM grafted from RAFT-Ph-MSNs.....	142
Figure 4.4	FESEM micrograph for a) PAM-COOH-MSNs having spherical morphology and b) PAM-Ph-MSNs having short-rod morphology.....	144
Figure 4.5	TEM micrographs for a) PAM-COOH-MSNs and b) PAM-Ph-MSNs.....	145

Figure 4.6	N ₂ 77 K adsorption (solid lines) and desorption (empty lines) isotherms and pore size distribution for PAM-COOH-MSNs (■) and PAM-Ph-MSNs (▲).....	146
Figure 4.7	FTIR spectra for a) AB nanoconfined into the pores of PAM-COOH-MSNs and b) AB nanoconfined into the pores of PAM-Ph-MSNs and compared with neat AB.....	147
Figure 4.8	Solid-state ¹¹ B NMR for AB nanoconfined into PAM-COOH-MSNs and PAM-Ph-MSNs.....	148
Figure 4.9	XRD pattern for control MSNs, PAM grafted MSNs, before and after AB incorporation.....	149
Figure 4.10	TPD-MS for hydrogen release from AB nanoconfined in polymer-grafted MSNs and neat AB. The dehydrogenation temperature for AB-PAM-COOH-MSNs was observed at 98°C and AB-PAM-Ph-MSNs was observed at 111°C in comparison to neat AB at 115°C.....	150
Figure 4.11	Co-relation between temperature reduction and pore size for AB confined PAM grafted MSNs with respect to neat AB.....	151
Figure 4.12	Dehydrogenation kinetics for (a) AB-PAM-COOH-MSNs at 70°C, 80°C and 90°C. (b) AB-PAM-COOH-MSNs at 70°C, 80°C and 90°C.....	153
Figure 4.13	Activation energies derived from Arrhenius plot for AB nanoconfined in PAM-COOH-MSNs and PAM-Ph-MSNs with rate constant (k) for the respective dehydrogenation temperatures.....	153
Figure 4.14	Wide scan XPS spectra for AB confined PAM-COOH-MSNs and deconvoluted narrow scan for boron (B 1s).....	156
Figure 4.15	Wide scan XPS spectra for AB confined PAM-Ph-MSNs and individual deconvoluted narrow scan for boron (B 1s).....	157
Figure 4.16	TPD-MS for (a) ammonia release, and (b) diborane release for both polymer-grafted MSNs.....	158

LIST OF TABLES

Table 2.1	Step-wide weight loss for control-MSNs, RAFT-COOH-MSNs ₆ , RAFT-COOH-MSNs _{12.8} and RAFT-COOH-MSNs ₁₈	71
Table 2.2	Step-wide weight loss for control-MSNs, RAFT-Ph-MSNs ₆ , RAFT-Ph-MSNs _{12.8} and RAFT-Ph-MSNs ₁₈	75
Table 2.3	BET and BJH analysis for all samples of RAFT functionalized MSNs...	82
Table 3.1.	Molecular weight of PNIPAM at different time interval of polymerization by surface initiated RAFT polymerization.....	98
Table 3.2	¹³ C assignments from solid state NMR spectra for PNIPAM grafted MSNs.....	101
Table 3.3	Weight loss for control-MSNs, RAFT-COOH-MSNs, and PNIPAM-COOH-MSNs.....	103
Table 3.4	Grafting ratio for both organoalkoxysilane RAFT agent and polymer on the surface of MSNs.....	105
Table 3.5	Textural properties of PNIPAM grafted MSNs in comparison to RAFT-COOH-MSNs.....	106
Table 3.6	Molecular weight for PAA chains grafted from both RAFT functionalized MSNs.....	109
Table 3.7	¹³ C assignments from solid state NMR spectra for PAA grafted MSNs...	112
Table 3.8	Weight loss for control-MSNs, RAFT functionalized MSNs and PAA grafted MSNs.....	114
Table 3.9	Grafting ratio for both organoalkoxysilane RAFT agent and polymer on the surface of MSNs.....	115
Table 3.10	Textural properties of PAA grafted MSNs in comparison to RAFT-COOH-MSNs.....	117

Table 3.11	Loading efficiency % for PAA and PNIPAM grafted MSNs.....	120
Table 3.12	Release efficiency % for PNIPAM grafted MSNs at 20°C, 30°C and 40°C	121
Table 3.13	Release efficiency % for PNIPAM grafted MSNs at 20°C, 30°C and 40°C	123
Table 4.1	a) ¹³ C assignments from the solid state NMR spectra for PAM-COOH-MSNs, b) ¹³ C assignments from the solid state NMR spectra for PAM-Ph-MSNs.....	143
Table 4.2	Weight loss for control-MSNs, RAFT functionalized MSNs and PAM grafted MSNs.....	145
Table 4.3	Textural properties of PNIPAM grafted MSNs in comparison to RAFT-COOH-MSNs.....	148

LIST OF ABBREVIATION

AIBN	Azobisisobutyronitrile
ATRA	Atom transfer radical addition
ATRP	Atom transfer radical polymerization
CMC	Critical micellar concentration
CRP	Controlled radical polymerization
CTAB	Cetyltrimethylammonium bromide
CTAB	Cetyltrimethylammonium bromide
DMEM	Dulbecco's modified Eagle's medium
DMF	Dimethylformamide
DOX	Doxorubicin
FBS	Fetal bovine serum
FTIR	Fourier-transform infrared
GSH	Glutathione
HRTEM	High resolution transmission electron microscopy
H-K	Horváth-Kawazoe
IUPAC	International Union of Pure and Applied Chemistry
LCST	Lower critical solution temperature
LCT	Liquid crystal template ²⁶
MAO	Methylaluminoxane
MAS	Magic angle spinning
MCM	Mobil crystalline materials

MSNs	Mesoporous silica nanoparticles
NMP	Nitroxide mediated polymerization
NMR	Nuclear Magnetic Resonance
PAH	Poly(allylamine hydrochloride)
PBS	Phosphate-Buffer Saline
PEGMA	poly(ethyleneglycol)methyl acrylate
PGMA	Poly(glycidyl methacrylate))
PMAA	Poly(methacrylic acid)
PMD	Periodic mesoporous z dendrisilicas
PMOs	Periodic mesoporous organosilicas
PNIPAM	Poly(N-isopropylacrylamide)
PNIPAM	Poly(N-isopropyl acrylamide)
Pen Strep	Penicillin–streptomycin
RAFT	Reversible addition-fragmentation chain transfer
SBA	Santa Barbara amorphous
SEC	Size exclusion chromatography
SEM	Scanning electron microscopy
STF	Shear thickening fluids
TEOS	Tetraethoxysilane
TEOS	Tetraethyl orthosilicate
THF	Tetrahydrofuran
TMOS	Tetramethyl orthosilicate
TPD-MS	Temperature programmed desorption-mass spectrometry

TPOS	Tetrapropyl orthosilicate
UV-Visible	Ultraviolet-Visible
XPS	X-ray photoelectron spectroscopy
XRD	X-ray diffraction